# Water/Polymer Interactions in a Poly(amidoamine) Hydrogel Studied by NMR Spectroscopy

Lucia Calucci,[†] Claudia Forte,*[,†] and Elisabetta Ranucci[‡]

*Istituto per i Processi Chimico-Fisici del CNR, Area della Ricerca di Pisa, via G. Moruzzi 1, 56124 Pisa, Italy, and Dipartimento di Chimica Organica e Industriale, via Venezian 21, 20133 Milano, Italy*

*Received April 17, 2007; Revised Manuscript Received June 21, 2007*

Samples of PAAH1, a cross-linked polymer belonging to the family of poly(amidoamine)s, were investigated at different hydration levels by means of $^{13}C$ and $^{1}H$ NMR techniques in order to obtain information on water/polymer interactions. Carbonyl oxygens and amine nitrogens were identified as the main sites of interaction giving hydrogen bonding with water molecules. The polymer turned out to be uniformly plasticized already at moderate degrees of swelling. The hydration process was found to occur in a stepwise manner, with the first batch of water saturating a hydration layer and additional water filling the polymer meshes. The proportion of water in the different states was quantitatively determined.

## Introduction

Ever since the first synthetic hydrogels were reported,[1] hydrogels have found wide application in biology and biomedicine, as soft contact lenses, drug delivery systems, implant materials, and tissue scaffolding.[2,3] Since water represents a significant proportion of swollen hydrogels, the status of water in these materials and the interaction of water with the polymer is fundamental in determining many of the gel properties, ranging from biocompatibility to the transport of small molecules. It is therefore not surprising that the physicochemical characterization of water in hydrogels has been the subject of numerous theoretical and experimental studies.

Among the different experimental techniques used to this aim, NMR has proven to be fundamental in characterizing the dynamics of water molecules and in highlighting water−polymer interactions, particularly through measurement of $^{1}H$ spin−lattice ($T_1$) and spin−spin ($T_2$) relaxation times as well as self-diffusion coefficients.[4] In polymeric hydrogels, where the polymer dynamics is strongly influenced by the water plasticizing effect and, at the same time, the boundaries constituted by the polymer network render the water motion anisotropic and more constrained, $^{1}H$ $T_1$ and $T_2$ relaxation times, which are determined by the modulation of magnetic interactions due to molecular motions, are expected to be very informative. However, it must be borne in mind that, in complex systems such as hydrogels, relaxation data analysis is not straightforward since magnetization transfer between polymer and water protons via chemical exchange and/or cross-relaxation can occur and must therefore be taken into account.[5]

NMR spectroscopy can also give site-specific information on the influence of hydration on polymer dynamics through $^{13}C$ cross-polarization (CP) and direct excitation (DE) magic-angle spinning (MAS) experiments. Whereas the former enhances signals arising from carbons strongly dipolarly coupled to protons, typically $^{13}C$ nuclei directly bonded to protons and in a rigid environment, the latter, performed with a very short recycle delay (on the order of seconds), shows only fast-relaxing carbon nuclei, usually located in quite mobile environments.

In this work, both $^{1}H$ and $^{13}C$ NMR techniques were used to characterize the water and polymer dynamics of PAAH1 (Figure 1), a cross-linked polymer belonging to the family of poly(amidoamine)s (PAAs). PAAs, obtained by Michael-type polyaddition of primary or secondary amines to bis-acrylamides,[6,7] contain tertiary amino and amido groups regularly arranged along the polymer chain. Cross-linked PAAs, which can be obtained using multifunctional amines as cross-linking agents, are typical hydrogels, absorbing large amounts of water when the cross-linking degree is not too high.[8] According to recent studies, PAA-based hydrogels are biodegradable and biocompatible substrates for cell culturing, showing, therefore, potential as a scaffold for tissue engineering.[9,10] Their investigation can therefore be considered of interest from both the academic and practical points of view.

PAAH1, obtained from the polyaddition of 2-methylpiperazine to 1,4-bis(acryloyl)piperazine with 20% 1,2-diaminoethane as the cross-linking agent,[11] was investigated both in the dry state and at different hydration levels in a wide range around its swelling ratio, which is 500%. A $CH_3COOH/CH_3COONa$ buffer (pH = 5.4) was used in order to guarantee hydrogel sample stability; in fact, PAAs can be indefinitely stored at acidic pH, whereas they slowly degrade at pH > 8.0.[12] It must be pointed out that PAAs do not behave as polyelectrolytes, and therefore the basicity constants of the aminic groups within the polymer correspond to those of the single moieties. According to protonation constants of 2-methylpiperazine ($pKa_1 = 7.15$, $pKa_2 = 3.14$) and 1,2-diaminoethane ($pKa_1 = 7.5$, $pKa_2 = 3.2$),[13] at pH = 5.4 about 98% of PAAH1 aminic nitrogens are monoprotonated. Consequently $NH^+$ groups can be considered, together with carbonyl oxygens, the main sites of interaction between water and the polymer chain via hydrogen bonding.

$^{13}C$ MAS experiments, both CP and DE with long and short recycle delay, were performed on all samples in order to highlight site-specific effects of hydration on polymer mobility. On the other hand, $^{1}H$ spin−spin ($T_2$) and spin−lattice ($T_1$) relaxation time analysis allowed information on both polymer

* Corresponding author. Address: Istituto per i Processi Chimico Fisici, CNR, Area della Ricerca di Pisa, via G. Moruzzi 1, 56124, Pisa, Italy. E-mail: c.forte@ipcf.cnr.it. Phone: +39-50-3152462.

[†] Istituto per i Processi Chimico-Fisici del CNR.

[‡] Dipartimento di Chimica Organica e Industriale.

10.1021/bm070417y CCC: $37.00 
Published on Web 08/24/2007

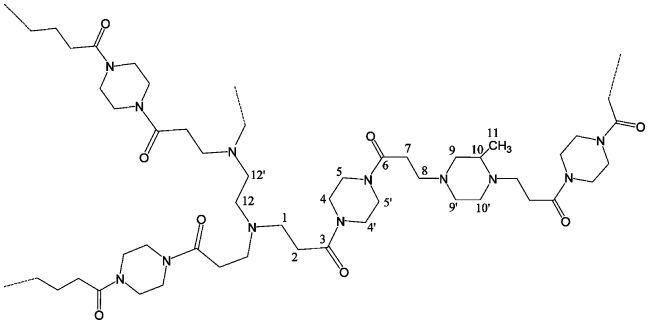

**Figure 1.** Structure of PAAH1.

and water dynamics to be obtained. Moreover, samples with different amounts of water were considered in order to elucidate the mechanism of the hydration process.

## Materials and Methods

**Materials.** PAAH1 was synthesized by the polyaddition of 2-methylpiperazine to 1,4-bis(acryloyl)piperazine with 1,2-diaminoethane in a molar ratio of 8:10:1, as reported in ref 11.

**Swelling Tests.** Swelling tests were carried out on polymer sheets with dimensions 10 × 20 × 1 $mm^3$ and an average weight of 20 mg. Each specimen, of initial mass $M_0$ was placed inside a 10 mL test tube containing 5 mL of water at 37 °C. After 12 h, the specimen was taken out of the test tube and weighed after wiping off any visible surface moisture. The swelling ratio (s.r.) was calculated using eq 1:

$$\text{s.r.}\% = \frac{M_s}{M_0} \times 100 \tag{1}$$

where $M_s$ is the swollen polymer weight.

**NMR Sample Preparation.** Hydrated samples were prepared by weighing PAAH1 in the MAS rotors and adding appropriate amounts of $CH_3COOH/CH_3COONa$ buffer (pH = 5.4). The samples were allowed to equilibrate for at least 12 h. Possible loss of water was checked by weighing the sample before and after swelling and NMR measurements. Six samples were prepared containing the following amounts of buffer: (**I**) 66.8 wt %, (**II**) 70.3 wt %, (**III**) 75.2 wt %, (**IV**) 80.0 wt %, (**V**) 85.5 wt %, and (**VI**) 89.8 wt %.

**NMR Measurements.** The NMR experiments were carried out on a Bruker AMX-300 WB spectrometer, working at 300.13 MHz for proton and at 75.47 MHz for carbon-13, equipped with a 4 mm CP-MAS probehead. All experiments were performed at 25 °C.

$^1$H MAS spectra were recorded with 16 scans, using a recycle delay of 10 s; the 90° pulse length was 4 $\mu$s. $^{13}$C CP-MAS experiments were carried out under $^1$H decoupling conditions using a recycle delay of 10 s and a contact time of 1 ms for the hydrated samples and 800 $\mu$s for the dry sample. In the $^{13}$C DE-MAS experiments, a recycle delay of 60 s was used, except in the case of selection of the fast relaxing components where a delay of 1 or 6 s was used. The 90° pulse length was 3.3 $\mu$s, and the MAS frequency was 6 kHz for the dry sample and 3 kHz for the hydrated samples.

Low-resolution $^1$H experiments were performed on-resonance on static samples. The 90° pulse length was 4 $\mu$s, the recycle delay was 10 s, and the number of scans accumulated was 16 for all experiments. For dry PAAH1, the $^1$H transverse magnetization decay was recorded using the solid echo pulse sequence[14] ($\pi/2_x$-$\tau$-$\pi/2_y$-$\tau$) with an echo delay of 16 $\mu$s and a dwell time of 1 $\mu$s. Transverse relaxation times of hydrated PAAH1 samples were determined from free induction decay (FID) for short times (on the order of a few hundreds of microseconds) and from echo values collected using the Carr−Purcell−Meiboom−Gill (CPMG) pulse sequence[15] ($\pi/2_x$-($\tau$-$\pi_y$-$\tau$)$_n$) with a time interval $\tau$ of 100 $\mu$s for longer times. For dry PAAH1, proton spin−lattice relaxation times in the laboratory ($T_1$) and rotating ($T_{1\rho}$) frames were measured using the inversion recovery pulse sequence followed by a solid-echo and the $\pi/2$-spin-lock solid-echo sequence with a 38 kHz spin-lock field, respectively, taking the magnetization intensity from the echo maximum. For the hydrated samples, the $^1$H spin−lattice relaxation time $T_1$ was measured using the inversion recovery pulse sequence.

**Data Analysis.** Inversion recovery curves, built with at least 25 points, were analyzed with a nonlinear least-squares fitting procedure. For dry PAAH1, the magnetization recovery was reproduced with the standard function

$$I(t) = I_\infty(1 - 2e^{-t/T_1}) \tag{2}$$

where $I(t)$ and $I_\infty$ are the spectral intensities at times t and ∞, respectively, and $T_1$ is the spin−lattice relaxation time. For samples **I**−**VI**, a sum of two exponential functions was required:

$$I(t) = I_\infty\{1 - 2[P_s e^{-t/T_{1s}} + (1 - P_s)e^{-t/T_{1l}}]\} \tag{3}$$

where $T_{1s}$ and $T_{1l}$ are the two spin−lattice relaxation times, and $P_s$ is the proton fractional population associated with $T_{1s}$.

The magnetization decay from the variable spin-lock experiment on dry PAAH1 was fitted using a biexponential function:

$$I(t) = I_0 \sum_i P_i e^{-t/T_{1\rho i}} \tag{4}$$

where $I_0$ is the echo maximum at time 0, and $T_{1\rho i}$ and $P_i$ are the spin−lattice relaxation time in the rotating frame and proton fractional population characterizing the *i*th component, respectively.

In order to reproduce the transverse magnetization decays, nonlinear least-squares fittings of acquired data were carried out using a linear combination of suitable analytical functions.[16] For dry PAAH1, the best results were obtained by using a weighted sum, $I(t)$, of an exponential, $E(t)$, and a Pake, $P(t)$, function:

$$I(t) = P_E E(t) + P_P P(t) \tag{5}$$

The exponential function $E(t) = e^{-t/T_2}$ is characterized by the spin−spin relaxation time $T_2$, whereas the Pake function can be written as[17,18]

$$P(t) = \sqrt{\frac{\pi}{6}}\, e^{-\beta^2 t^2/2}\left[\frac{\cos \alpha t}{\sqrt{\alpha t}}\, C\left(\sqrt{\frac{6\alpha t}{\pi}}\right) + S\left(\sqrt{\frac{6\alpha t}{\pi}}\right)\frac{\sin \alpha t}{\sqrt{\alpha t}}\right] \tag{6}$$

where $C$ and $S$ are approximated Fresnell functions,[19] and $\alpha = 3\gamma^2\hbar/4R_{HH}^3$, with $\gamma$ being the proton gyromagnetic ratio. The Pake function is therefore characterized by the parameters $R_{HH}$, the distance between two nearest neighbor protons, and $\beta$, a parameter related to the dipolar interactions between two non-nearest neighboring protons. For hydrated PAAH1 samples, the best fit of the FIDs were obtained with a mono- or biexponential function of the type of eq 4, where $T_2$ is used instead of $T_{1\rho}$. Analogous functions were used for the fitting of CPMG curves.

For the discussion of the data, water and polymer proton populations were estimated from the composition of the different samples; in the calculations, polymer vinyl dangling ends and unreacted 1,2-diaminoethane NH functions were neglected on the basis of the findings of ref 11 and of the $^{13}$C MAS spectra.

## Results

**$^{13}$C MAS NMR.** $^{13}$C CP- and DE-MAS experiments with different recycle delays were recorded on dry PAAH1 (see Figure 2). Four groups of signals can be distinguished in all the spectra: two relatively sharp peaks at 17.8 and 170.3 ppm

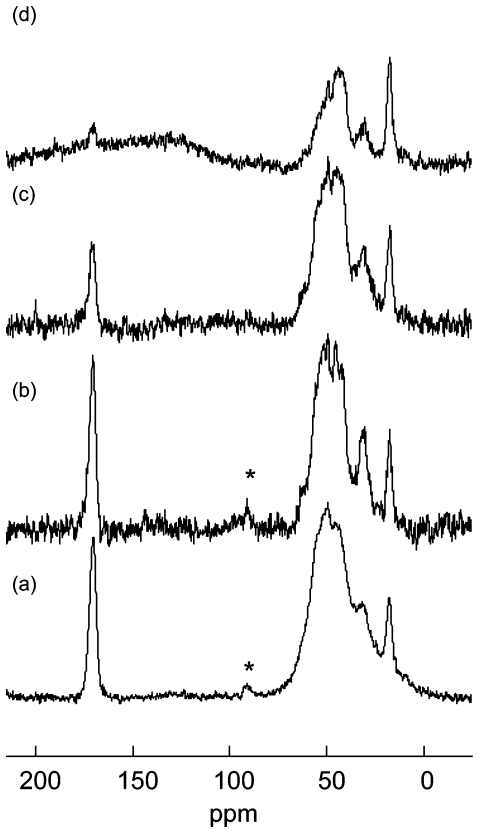


**Figure 2.** $^{13}$C CP-MAS (a) and DE-MAS (b−d) spectra of dry PAAH1 polymer. DE-MAS spectra were recorded with a recycle delay of 60 s and 1000 scans (b), 6 s and 1200 scans (c) and 1 s and 1200 scans (d). 2000 scans were acquired for the CP-MAS spectrum. The asterisk indicates a spinning side band.

ascribable to methyl and carbonyl carbons, respectively; a peak at about 32 ppm due to methylene carbons 2 and 7 (see Figure 1); and a broad signal between 35 and 75 ppm due to all the remaining carbons.[11]

By comparing the signal intensities in the different spectra, it can be seen that, besides methyl carbons, which are expected to undergo fast relaxation, signals in the region 28−46 ppm are also observed in the short recycle delay DE spectrum, indicating a faster relaxation for the corresponding carbons with respect to the remaining ones.

Upon hydration, thanks to the plasticizing and homogenizing effect of water, the $^{13}$C spectral resolution is greatly enhanced, as shown in Figure 3 for sample **IV**. In this case, a spectral deconvolution yielded chemical shifts and relative intensities of all signals which, compared with HR-MAS data,[11] allowed a full spectral assignment to be made (see Table 1). It is worthy of note that the differences in chemical shift values with respect to those obtained from HR-MAS experiments in dimethylformamide (DMF)-$d_7$ are significant (0.6−2.5 ppm) for all carbons except for the methyl and 1,4-bis(acryloyl)piperazine ring ones. No differences in chemical shifts have been observed for PAAH1 samples at different hydration levels. The $^{13}$C signals due to vinyl dangling ends at 127.2 and 128.9 ppm were observed only in experiments with a high number of scans (>20 000), in agreement with their low quantity (less than 4%).[11]

Comparison between spectra recorded under CP and DE conditions (Figure 3) indicates that the polymer mobility is sensibly increased upon hydration. In fact, even in the least hydrated sample (**I**), the short recycle time (1 s) DE spectrum shows 70% of the signal intensity of the long recycle time (60 s) DE spectrum; moreover, its CP spectrum has an overall

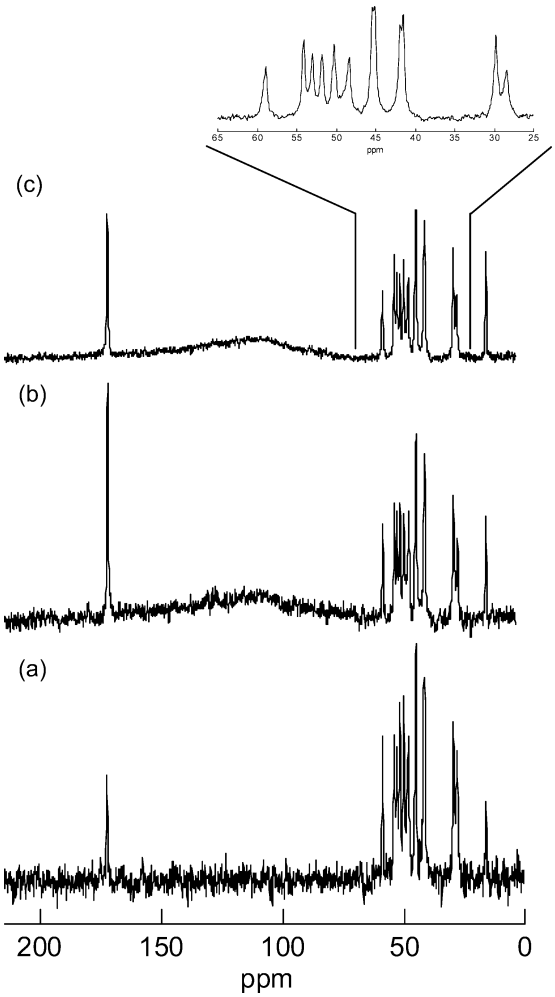


**Figure 3.** $^{13}$C CP-MAS (a) and DE-MAS (b,c) spectra of hydrated PAAH1 (sample **IV**). DE-MAS spectra were recorded with a recycle delay of 60 s and 3000 scans (b) and 1 s and 16000 scans (c); 4000 scans were acquired for the CP-MAS spectrum.

**Table 1.** Assignment of the $^1$H and $^{13}$C NMR Spectra of PAAH1

| $^{13}$C | | | $^1$H | |
|---|---|---|---|---|
| C[a] | $\delta$ (ppm) | $\delta$ (ppm)[b] | H[a] | $\delta$ (ppm) |
| 11 | 16.2 | 16.8 | 11 | 1.13 |
| 2 (7) | 28.4 | 30.95 | 9 | 1.94 |
| 7(2) | 29.7 | 30.95 | 1,2,7,8,9′,10,10′ | 2.0−3.2 |
| 4,4′ (5,5′) | 41.5, 41.9 | 41.3, 41.8 | 4,5,4′,5′ | 3.67 |
| 5,5′ (4,4′) | 45.1, 45.4 | 45.4, 45.7 | | |
| 1 | 48.3 | 49.6 | | |
| 12,12′ | 48.9 | 50.5 | | |
| 10′ | 50.2 | 51.6 | | |
| 9′ | 51.8 | 53.8 | | |
| 8 | 53.0 | 54.4 | | |
| 10 | 54.1 | 54.7 | | |
| 9 | 58.9 | 61.3 | | |
| 3,6 | 172.6, 172.8 | 170.4, 170.7 | | |

[a] The numbering is shown in Figure 1. [b] Measured in DMF-$d_7$ by HR-MAS in ref 11.

intensity of only ∼10% of that expected assuming ideal CP conditions. A detailed analysis highlights that, within each spectrum, the relative signal intensities do not show differences except for the methyl and carbonyl carbons, indicating that hydration affects all the polymer moieties uniformly. Methyl groups, undergoing fast rotation around their ternary axes, show, as expected, a different behavior, yielding an enhanced signal

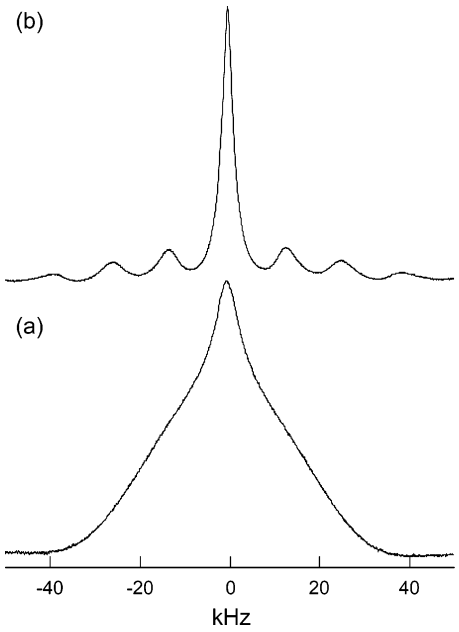


**Figure 4.** $^1$H static (a) and 12 kHz MAS (b) NMR spectra of dry PAAH1.

in the short recycle time DE spectrum and a reduced one in the CP spectrum. As far as the carbonyl carbons are concerned, their signal is relatively smaller in the CP and, to a minor extent, in the DE spectrum at short recycle time; these effects are ascribable to the absence of directly bonded protons, which largely contribute to both cross-polarization and relaxation.

**$^1$H MAS NMR.** The static $^1$H spectrum of dry PAAH1 (Figure 4) clearly reveals the presence of a broad component extending over 75 kHz and a narrower one with a line width of ~10 kHz. In the spectra recorded under MAS conditions (Figure 4), at spinning rates higher than 8 kHz, a splitting of the broader signal into spinning sidebands is observed, ascribable to the inhomogeneous component of the homonuclear dipolar interaction.[20] For this type of sample, $^1$H spectra are, however, quite uninformative; more detailed quantitative information can be obtained from transverse magnetization decay analysis, described in the following section.

Hydration resulted in a significant narrowing of the $^1$H static spectra, confirming increased mobility; spectra recorded under MAS conditions, even at low spinning speeds (500 Hz), showed resolved signals for water and polymer protons, allowing the sample composition to be verified. However, the spectral resolution was not good enough to obtain site-specific information given the strong overlap of polymer proton signals. A gross assignment, performed on the basis of literature data,[11] is reported in Table 1.

**$^1$H Relaxation.** The on-resonance $^1$H echo decay of dry PAAH1 is shown in Figure 5: at least two decay curves can be distinguished, corresponding to the two components observed in the static spectrum. In fact, the experimental decay could be well reproduced using a linear combination of an exponential and a Pake function (see experimental section for details), describing a slower and a faster magnetization decay, respectively (Figure 5). The best fitting Pake function, contributing 78 ± 1% to the signal intensity, is characterized by $R_{HH} = 1.78 \pm 0.01$ Å, close to H−H distances in methylene groups, and $\beta = 65 \pm 1$ kHz, corresponding to a spin−spin relaxation time of ~20 $\mu$s. On the other hand, the best-fit exponential function is characterized by a $T_2$ value of 46 ± 1 $\mu$s. This result was confirmed by $^{13}$C delayed CP-MAS experiments where contributions from protons with $T_2$ shorter than the experimental delay used are sensibly reduced; for PAAH1, a delay of 15 $\mu$s gave a spectrum with intensity reduced by 75%. It must be pointed out that the signal reduction concerned all carbons to the same extent, indicating that the two different $^1$H decay components are not ascribable to specific polymer moieties.

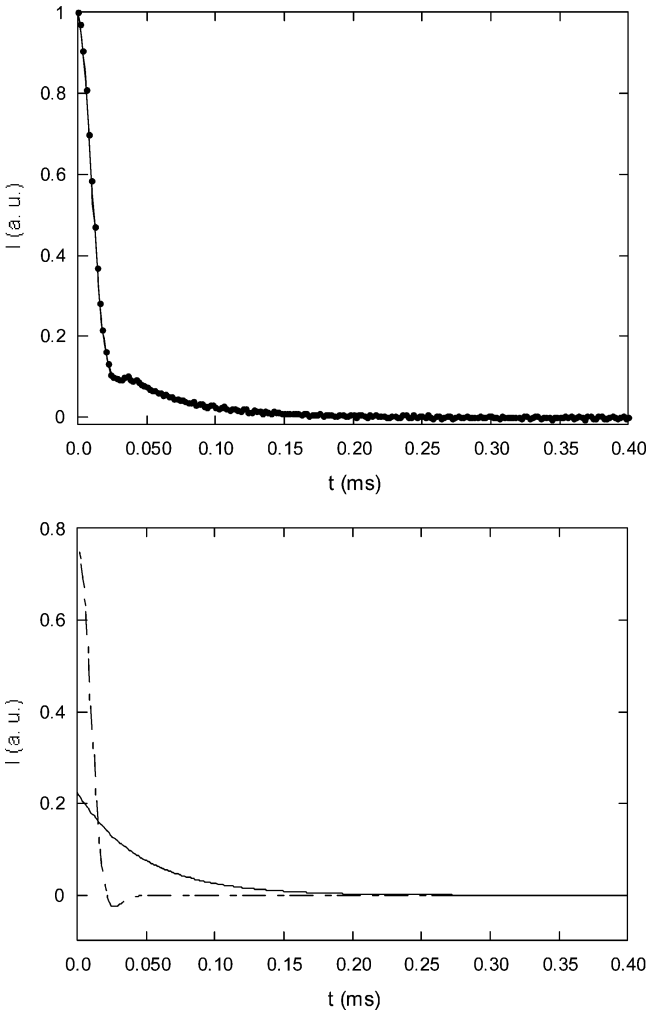


**Figure 5.** Top: experimental (points) and best-fit calculated (line) $^1$H transverse magnetization decay of dry PAAH1. Bottom: best-fit exponential (solid line) and Pake (dashed line) functions. Only the first 400 points of the decay are shown.

The dry PAAH1 proton spin−lattice relaxation times in the laboratory ($T_1$) and rotating ($T_{1\rho}$) frames were also measured; the magnetization recovery in the inversion recovery experiment was well fitted by a single exponential function characterized by $T_1 = 2.15 \pm 0.01$ s, whereas the magnetization decay in the variable spin-lock experiment required two exponential functions with $T_{1\rho} = 1.1 \pm 0.2$ ms and $3.7 \pm 0.2$ ms, respectively.

For hydrated PAAH1 samples, because $T_2$ values differing by orders of magnitude (from tens of microseconds to seconds) could be present, the determination of proton spin−spin relaxation times required a combination of FID analysis and CPMG experiments. In fact, the former is suitable for measuring relaxation times shorter than 1 ms, whereas the latter is necessary for a correct determination of longer components, thus avoiding field inhomogeneity effects.

For samples **I** and **II**, the FID (Figure 6) was well reproduced by a single exponential function with a $T_2$ value of about 550 $\mu$s; for the remaining samples, two exponential functions had to be used: one characterized by a $T_2$ value similar to that

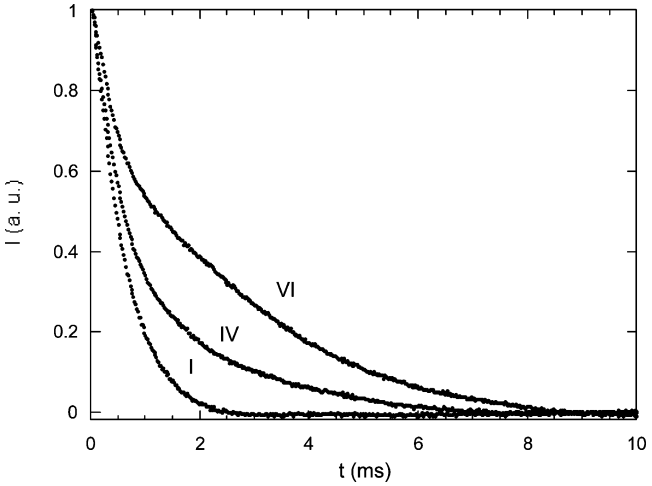


**Figure 6.** First 5000 points of $^1$H FIDs of samples **I**, **IV**, and **VI**.

observed for samples **I** and **II** ($T_{2s}$ in Table 2), the other with a $T_2$ value on the order of a few milliseconds. Given the limitations of the technique mentioned above, only the $T_2$ and relative population of the fast decaying component were considered from this analysis (Table 2). It must be pointed out that, in the case of samples **I** and **II**, the fitting of the FID with a single exponential function does not exclude the presence of a small proportion of slow decaying component; in fact, a mathematical simulation showed that the fitting with a monoexponential function remains acceptable with a $T_2$ component of a few milliseconds contributing at most 10% to the FID.

CPMG curves could be satisfactorily reproduced by the sum of two exponential decay functions for samples **I**−**V**, whereas three exponential components were required for sample **VI**. In all cases, the faster decaying component, which is due to residual magnetization of the short $T_2$ component of the FID, shows an apparent $T_2$ of few milliseconds, differing from its true value because of the CPMG sequence timing. The slow decaying component is characterized by a $T_2$ value ($T_{2l}$ in Table 2) of ∼500 ms for samples **I**−**III** and of 760 and 960 ms for samples **IV** and **V**, respectively; a similar component with $T_2 \cong 500$ ms was found in sample **VI** where, however, the main component was an additional one with a $T_2$ value of 2.18 s ($T_{2f}$ in Table 2). The increase in $T_{2l}$ observed for samples **IV** and **V** with respect to samples **I**−**III**, is to be ascribed to the presence of another component in the CPMG decay with a $T_2$ value on the order of $T_{2f}$ but in such a low quantity that it remains undistinguished in the fitting procedure.

As far as $^1$H spin−lattice relaxation is concerned, the inversion recovery curves of hydrated PAAH1 samples obtained from the first point of the FIDs could be satisfactorily reproduced with a sum of two exponential functions; the shortest time constant ($T_{1s}$) is in all cases on the order of 300 ms, whereas the longest one ($T_{1l}$, reported in Table 2) increases with increasing water content from 800 ms to ∼2 s, with the corresponding proton population increasing from 67 to 89%. On the other hand, the inversion recovery curves obtained using a point of the FIDs at 800 $\mu$s, where the contribution of the short $T_2$ component is sensibly reduced, could always be fitted by a monoexponential function with a $T_1$ equal to $T_{1l}$.

## Discussion

Both $^1$H FID analysis and $^{13}$C MAS experiments pointed out that PAAH1 is a quite rigid polymer. In particular, a very rigid component, well described by a Pake function, accounts for the majority (78%) of PAAH1 protons, whereas the remaining protons are in a less (but still) rigid environment ($T_2$ on the order of 50 $\mu$s). The Pake function, characterized by $R_{HH} = 1.78$ Å, a distance close to that between protons in a methylene group, and $\beta = 65$ kHz, corresponding to a $T_2$ value of about 20 $\mu$s, indicates that spin−spin relaxation is mainly due to neighboring proton dipolar interactions modulated by slow polymer motions. No resolution of the $^1$H spectrum was achieved by spinning the sample at rates up to 12 kHz, even though the broader spectral component splits into spinning sidebands for spinning rates higher than 8 kHz. This can be justified on the basis of the inhomogeneous nature of the main interaction, i.e., the dipolar coupling between neighboring protons expected to be on the order of 20 kHz. On the other hand, partial spectral resolution was obtained by MAS rotation in $^{13}$C experiments, even though the residual line broadening suggests structural heterogeneity ascribable to the amorphous character of PAAH1. The $^{13}$C CP- and DE-MAS spectra allowed us to infer that, apart from methyl groups, which are very mobile, methylene groups adjacent to carbonyls and those of the 1,4-bis(acryloyl)piperazine ring, giving rise to signals in the region 28−46 ppm, undergo faster motions with respect to the remaining groups. The spin−lattice relaxation times $T_1$ and $T_{1\rho}$ can be used to obtain information on the degree of spatial heterogeneity in dry PAAH1, exploiting the phenomenon of spin diffusion;[21] in fact, the averaging effect of spin diffusion is complete in the $T_1$ but not in the $T_{1\rho}$ time scale, allowing a rough estimate of the homogeneous domains' maximum size to be made on the basis of the following equation:

$$\langle r^2 \rangle = 6D\tau \qquad (7)$$

where a spherical model is assumed for the domains with radius $r$, $D$ is the diffusion coefficient, taken here equal to $10^{-16}$ m$^2$ s$^{-1}$, a value valid for dense rigid proton systems,[22] and $\tau$ is the time required for the magnetization exchange between two spins in the Gaussian random walk model on which eq 7 is based. Equating $\tau$ with $T_1$ for our sample, a value for $r$ of ∼300 Å was obtained.

When hydrated, PAAH1 shows increased dynamics, as indicated by the high resolution of $^1$H and $^{13}$C MAS spectra, which allow signal assignment to be performed, and by the $^1$H relaxation times measured. Nevertheless, the polymer maintains a certain degree of "solid-like" character, giving rise to efficient cross-polarization in CP experiments, in agreement with the picture of hydrogels as solids, although elastic. It must be pointed out that the enhanced dynamics indiscriminately concerns all polymer moieties since, apart from methyl groups, no differences in the relative intensity of the different peaks have been observed from the comparison of $^{13}$C CP- and DE-MAS spectra. On the other hand, appreciable variations in chemical shift were observed upon hydration for most but not all the $^{13}$C signals, indicating site-specific interactions of water with the polymer. In particular, the carbonyl carbons' chemical shifts show a downfield shift of ∼2 ppm with respect to both those reported in DMF solution and that observed in the dry state; shifts of this order of magnitude have been observed for carbonyl carbons in other polymer systems and ascribed to hydrogen bonding between water protons and C═O oxygens.[23] All the other carbons, with the exception of those of the 1,4-bis(acryloyl)piperazine ring, show up-field shifts in the range of 0.6−2.5 ppm, in agreement with variations observed for tertiary amines upon protonation.[24] These findings confirm the expected stronger interactions of water with C═O and $NH^+$ groups.

$^1$H FID analysis and spin−spin relaxation time measurement

**Table 2.** Spin−Lattice ($T_{1l}$) and Spin−Spin ($T_{2s}$, $T_{2l}$, $T_{2f}$) Relaxation Times with Corresponding Proton Populations (in parentheses) Determined for Hydrated PAAH1 Samples

| sample | water wt % | water proton % | $T_{1l}$ (s) (%) | $T_{2s}$ ($\mu$s) (%) | $T_{2l}$ (ms) (%) | $T_{2f}$ (s) |
|---|---|---|---|---|---|---|
| **I** | 66.8 ± 0.2 | 71.9 | 0.80 ± 0.01 (67 ± 3) | 580 ± 10 (>90) | 470 ± 10 | |
| **II** | 70.3 ± 0.2 | 75.1 | 0.88 ± 0.01 (70 ± 2) | 540 ± 10 (>90) | 490 ± 10 | |
| **III** | 75.2 ± 0.2 | 79.5 | 1.05 ± 0.01 (76 ± 1) | 600 ± 10 (75 ± 5) | 530 ± 10 | |
| **IV** | 80.0 ± 0.2 | 83.6 | 1.19 ± 0.01 (79 ± 1) | 430 ± 10 (53 ± 5) | 730 ± 10 | |
| **V** | 85.5 ± 0.2 | 88.2 | 1.51 ± 0.01 (83 ± 1) | 440 ± 10 (53 ± 5) | 960 ± 20 | |
| **VI** | 89.8 ± 0.2 | 91.8 | 2.04 ± 0.02 (89 ± 1) | 410 ± 10 (22 ± 3) | 510 ± 40 (39 ± 3) | 2.18 ± 0.08 |

by CPMG experiments revealed the presence of two main proton domains with $T_2$ values differing by 3 orders of magnitude for all hydrated samples, apart from sample **VI**, for which a third component with a $T_2$ value typical of free water ($T_{2f}$) was observed. The fast decaying component, on the basis of its $T_2$ value ($T_{2s} \sim 500$ $\mu$s) and the corresponding proton population, is to be ascribed to the polymer and to water molecules with restricted mobility, i.e., strongly interacting with the polymer. The second component, with $T_2$ on the order of hundreds of milliseconds ($T_{2l}$), is due to water with much higher mobility within the hydrogel structure, whereas the third component, observed for sample **VI**, and presumably also present in sample **V**, is due to free water outside the hydrogel. The contribution of PAAH1 protons to the short $T_2$ component is confirmed by $^{13}$C delayed CP-MAS experiments performed with different delays (results not shown), from which a $T_2$ on the order of 150 $\mu$s could be estimated.

Spin−lattice relaxation analysis yielded two relaxation times $T_{1s}$ and $T_{1l}$ for all hydrated samples, with $T_{1s}$ being practically constant (~300 ms) and $T_{1l}$ increasing, together with its relative population, with increasing water content. In heterogeneous samples, such as hydrogels, the observation of two $T_1$ values could be due to the presence of two proton domains either with negligible magnetization transfer or with cross-relaxation[25] and/or chemical exchange[26] at a rate comparable to $1/T_1$; in the former case, the different $T_1$ values can be associated with the two distinct proton domains, whereas, in the latter case, the two $T_1$'s determined, which should be the same for both domains, are apparent relaxation times related to the two intrinsic relaxation times and the rate of magnetization transfer. Although a small contribution of magnetization transfer cannot be excluded, in our case there is strong evidence that the two spin−lattice relaxation times measured are associated with two proton domains with different mobility. In fact, on the basis of the results obtained from different points of the FIDs (i.e., the first point and a point at 800 $\mu$s) and the proton populations corresponding to the two $T_1$ values, $T_{1s}$ can be ascribed to the polymer and hydrogen-bonded water molecules, and $T_{1l}$ can be ascribed to the remaining water. The proton population contributing to $T_{1s}$ indeed corresponds to the polymer fraction plus ~40 molecules of water per polymer unit, this unit being defined as the sum of ten 1,4-bis(acryloyl)piperazine, eight 2-methylpiperazine, and one 1,2-diaminoethane moieties. This number agrees well with the number of hydrogen-bonded water molecules expected per polymer unit considering the number of C═O and $NH^+$ groups. The fraction of water protons characterized by $T_{2s}$, aside from those of hydrogen-bonded molecules, presumably belongs to a hydration layer around the polymer chain with an estimated thickness on the order of few angstroms.

The different populations found for $T_{1l}$ and $T_{2l}$ can be explained in terms of the exchange of water molecules between the hydration layer, characterized by $T_{2s}$, and the hydrogel meshes, which should be fast in the $T_1$ time scale but not in the $T_2$ one. The averaging effect of water diffusion on spin−lattice relaxation times is often observed in swollen hydrogels.[27−30] Thus, assuming that the spin−lattice relaxation rate $1/T_{1l}$ results from a population weighted average of two limiting values ascribable to water in the hydration layer and free water, according to the two-fraction fast exchange model,[26] the measured relaxation rates can be expressed as:

$$\frac{1}{T_{1l}} = \frac{w_{hl}}{T_{1hl}} + \frac{w_f}{T_{1f}} \tag{8}$$

where $w_i$ and $T_{1i}$ are the proton populations and corresponding relaxation times of the hydration layer (hl) and free (f) water. Applying eq 8 with $T_{1f} = 2.18$ s, assumed to be equal to the $T_{2f}$ measured for water outside the hydrogel in sample **VI**, the linear dependence of $1/T_{1l}$ on $w_{hl}$ obtained for our samples could be well reproduced with $T_{1hl} = 800 \pm 50$ ms.

All this considered, the trend of proton populations and $T_1$ and $T_2$ values suggests a hierarchy of hydration: at low hydration levels (i.e., samples **I** and **II**), water distributes around the polymer chains until the hydration layer is saturated; additional water tends to enlarge the polymer meshes until the hydrogel is completely swollen and any further water remains outside (as in sample **VI**). The stepwise character of this process has been previously observed in cross-linked hydrogels by thermal measurements.[31,32]

## Conclusions

The combined application of $^{13}$C and $^1$H NMR techniques to a cross-linked PAA hydrogel in the dry state and hydrated with different amounts of water allowed us to shed light on the effects of the hydration process on both the polymer and water properties.

High-resolution $^{13}$C NMR experiments highlighted the plasticizing effect of water on the polymer chains, already observable at the lowest hydration level investigated, influencing all polymer moieties to the same extent, even though site-specific interactions occur between water and carbonyl oxygens as well as protonated amine nitrogens through hydrogen bonds, as

clearly indicated by chemical shift variations. The fraction of hydrogen-bonded water was confirmed by $^1$H spin−lattice relaxation measurements.

A thorough analysis of $^1$H spin−spin and spin−lattice relaxation times yielded information on water distribution in the hydrogel and showed that hydration occurs via a stepwise process in which a water layer around the polymer chains is first formed, and then water fills the polymer meshes, which are progressively enlarged.

## References and Notes


(1) Wichterle, O.; Lim, D. *Nature* **1960**, *185*, 117−118.
(2) Hoffman, A. S. *Adv. Drug Delivery Rev.* **2002**, *43*, 3−12.
(3) Peppas, N. A.; Hilt, J. Z.; Khademhosseini, A.; Langer, R. *Adv. Mater.* **2006**, *18*, 1345−1360.
(4) Mathur, A. M.; Scranton, A. B. *Biomaterials* **1996**, *17*, 547−557.
(5) McBrierty, V. J.; Martin, S. J.; Karasz, F. E. *J. Mol. Liquids* **1999**, *80*, 179−205.
(6) Ferruti, P.; Marchisio, M. A.; Barbucci, R. *Polymer* **1985**, *26*, 1336−1348.
(7) Ferruti, P. In *Polymeric Materials Encyclopedia*; Salamone, J. C., Ed.; CRC Press: Boca Raton, FL, 1996; Vol. 5, pp 3334−3359.
(8) Ferruti, P.; Marchisio, M. A.; Duncan, R. *Macromol. Rapid Commun.* **2002**, *23*, 332−355.
(9) Ferruti, P.; Bianchi, S.; Ranucci, E.; Chiellini, F.; Caruso, V. *Macromol. Biosci*. **2005**, *5*, 613−622.
(10) Ferruti, P.; Bianchi, S.; Ranucci, E.; Chiellini, F.; Piras, A. M. *Biomacromolecules* **2005**, *6*, 2229−2235.
(11) Annunziata, R.; Franchini, J.; Ranucci, E.; Ferruti., P. *Magn. Reson. Chem.* **2007**, *45*, 51−58.
(12) Ferruti, P.; Ranucci, E.; Sartore, L.; Bignotti, F.; Marchisio, M. A.; Bianciardi, P.; Veronese, F. M. *Biomaterials* **1994**, *15*, 1235−1241.
(13) Pesavento, M.; Soldi, T.; Ferruti, P.; Barbucci, R.; Benvenuti, M. *J. Appl. Polym. Sci.* **1983**, *28*, 3361−3368.
(14) Powles, J. G.; Strange, J. H. *Proc. Phys. Soc. London* **1963**, *82*, 6−15.
(15) Carr, H. Y.; Purcell, E. M. *Phys. Rev.* **1954**, *94*, 630−638. Meiboom, S.; Gill, D. *Rev. Sci. Instrum.* **1958**, *29*, 688−691.
(16) Hansen, E. W.; Kristiansen, P. E.; Pedersen, N. *J. Phys. Chem. B* **1998**, *102*, 5444−5450.
(17) Pake, G. E. *J. Chem. Phys.* **1948**, *16*, 327−336.
(18) Look, D. C.; Lowe, I. J.; Northby, J. A. *J. Chem. Phys.* **1966**, *44*, 3441−3452.
(19) Abramowitz, M.; Stegun, I. *Handbook of Mathematical Functions*; Dover: New York, 1970.
(20) Schnell, I.; Spiess, H. W. *J. Magn. Reson.* **2001**, *151*, 153−227.
(21) McBrierty, V. J.; Packer, K. J. *Nuclear Magnetic Resonance in Solid Polymers*; Cambridge University Press: Cambridge, U.K., 1993.
(22) Havens, J. R.; VanderHart, D. L. *Macromolecules* **1985**, *18*, 1663−1676.
(23) Keely, C. M.; Zhang, X.; McBrierty, V. J. *J. Mol. Struct.* **1995**, *355*, 33−46.
(24) Morishima, I.; Yoshikawa, K.; Okada, K.; Yonezawa, T.; Goto, K. *J. Am. Chem. Soc.* **1973**, *95*, 165−171.
(25) Edzes, H. T.; Samulski, E. T. *J. Magn. Reson.* **1978**, *31*, 207−229.
(26) Zimmerman, J. R.; Brittin, W. E. *J. Phys. Chem.* **1957**, *61*, 1328−1333.
(27) Barbucci, R.; Leone, G.; Chiumiento, A.; Di Cocco, M. E.; D'Orazio, G.; Gianferri, R.; Delfini, M. *Carbohydr. Res.* **2006**, *341*, 1848−1858.
(28) Tanaka, H.; Fukumori, K.; Nishi, T. *J. Chem. Phys.* **1988**, *89*, 3363−3372.
(29) Baohui, L.; Datong, D.; Yinong, W.; Pingchuan, S.; Jianbiao, M.; Binglin, H. *J. Appl. Polym. Sci.* **1999**, *72*, 1203−1207.
(30) McConville, P.; Whittaker, M. K.; Pope, J. M. *Macromolecules* **2002**, *35*, 6961−6969.
(31) Sung, Y. K.; Gregonis, D. E.; John, M. S.; Andrade, J. D. *J. Appl. Polym. Sci.* **1981**, *26*, 3719−3728.
(32) Coyle, F. M.; Martin, S. J.; McBrierty, V. J. *J. Mol. Liquids* **1996**, *69*, 95−116.


BM070417Y